Rathke cleft cysts: correlation of enhanced MR and surgical findings.

M Sumida, T Uozumi, K Mukada, K Arita, K Kurisu and K Eguchi

AJNR Am J Neuroradiol 1994, 15 (3) 525-532
http://www.ajnr.org/content/15/3/525

Rathke Cleft Cysts: Correlation of Enhanced MR and Surgical Findings

Masayuki Sumida, Tohru Uozumi, Kazutoshi Mukada, Kazunori Arita, Kaoru Kurisu, and Kuniki Eguchi

PURPOSE: To describe the gadolinium-enhanced MR findings of Rathke cleft cyst, correlate them with the surgical findings, and define those preoperative findings that differentiate this lesion from other sellar and juxtasellar tumors. **METHODS:** We studied 18 patients who were diagnosed as having Rathke cleft cyst pathologically. These patients were imaged with T1- and T2-weighted coronal and sagittal spin-echo sequences. Fifteen of these patients received gadopentetate dimeglumine. **RESULTS:** In eight patients, the cyst showed low intensity on T1-weighted images and high intensity on T2-weighted images. At surgery, the cyst fluid was cerebrospinal fluid–like or light brown in five patients, motor oil–like in one patient, and milky in two patients. In 10 patients, cysts showed isointensity to high intensity on T1-weighted images and had various intensity on T2-weighted images. All 10 contained milky fluid. In three patients the intensity of fluid was heterogeneous. A waxy nodule was found in two patients. The position of the normal pituitary gland confirmed by surgery in all cases coincided with enhancement on MR imaging. The variable position of the normal pituitary gland was clearly identified in the sagittal images. The cyst walls showed no enhancement by gadopentetate dimeglumine. **CONCLUSIONS:** Because Rathke cleft cysts show variable intensities on MR, the diagnosis is often difficult when based on MR signal intensity values alone. MR imaging with gadopentetate dimeglumine does assist in the diagnosis of Rathke cleft cysts. Diagnostic clues include the lack of cyst wall enhancement and displacement of the normal pituitary gland.

Index terms: Sella turcica, cysts; Sella turcica, magnetic resonance; Magnetic resonance, contrast enhancement

AJNR Am J Neuroradiol 15:525–532, Mar 1994

Rathke cleft cyst has long been regarded as a relatively infrequent sellar/juxtasellar tumor; nonetheless, its frequency in normal autopsies was reported to be as high as 13% to 22% (1, 2). In addition, an increasing number of cases have been reported, because of the use of computed tomography (CT) and magnetic resonance (MR) in diagnostic imaging. Because only cyst aspiration and partial removal of Rathke cleft cyst is regarded to be sufficient, and few recurrences have been reported, Rathke cleft cysts are approached surgically in a different manner than sellar and juxtasellar tumors such as pituitary adenoma and craniopharyngioma. Thus the preoperative diagnosis and differentiation from other sellar and juxtasellar tumors can be surgically important (3–6). We report our observations obtained from the correlation of MR imaging to surgical findings in 18 patients with Rathke cleft cysts. MR criteria for preoperative diagnosis are discussed.

Patients and Materials

We did a retrospective study of 18 patients in the Department of Neurosurgery at Hiroshima University and related hospitals during a 6-year period from April 1986 to March 1992 (Table 1). All patients had preoperative MR studies and were subsequently diagnosed by surgical pathology as having Rathke cleft cysts. The patients included 10 men and eight women, 17 to 74 years of age. Clinical symptoms were observed in 14 patients. These included visual disturbances or visual field defects in seven patients, endocrine symptoms such as diabetes insipidus in five, and

Received May 28, 1992; accepted pending revision August 13; revision received June 7, 1993.

From the Department of Neurosurgery, Hiroshima University School of Medicine, Japan.

Address reprint requests to Masayuki Sumida, MD, Department of Neurosurgery, Hiroshima University School of Medicine, 1–2–3 Kasumi, Minami-ku, Hiroshima, 734, Japan.

AJNR 15:525–532, Mar 1994 0195-6108/94/1503-0525

TABLE 1: Clinical findings in 18 Rathke cleft cysts

Case	Age/Sex	Symptoms	Lesion Size (mm)	Lesion Location	Surgical Approach
1	37/M	Headache	20 × 12 × 26	Intrasellar and suprasellar	Transsphenoidal
2	35/F	Amenorrhea	14 × 14 × 22	Intrasellar and suprasellar	Transsphenoidal
3	63/M	Visual disturbance	16 × 17 × 20	Intrasellar and suprasellar	Transcranial
4	40/M	Headache	9 × 12 × 9	Suprasellar	Transcranial
5	32/F	Visual disturbance	26 × 23 × 28	Intrasellar and suprasellar	Transsphenoidal
6	70/M	Diabetes insipidus Hypopituitarism	20 × 16 × 23	Intrasellar and suprasellar	Transcranial
7	70/F	Bitemporal hemianopsia	16 × 15 × 22	Intrasellar and suprasellar	Transcranial
8	71/M	Bitemporal hemianopsia	18 × 14 × 20	Intrasellar and suprasellar	Transcranial
9	41/M	Bitemporal hemianopsia	14 × 16 × 26	Intrasellar and suprasellar	Transsphenoidal
10	21/F	Amenorrhea Galactorrhea	18 × 5 × 12	Intrasellar	Transsphenoidal
11	63/M	Hypopituitarism	17 × 16 × 18	Intrasellar and suprasellar	Transsphenoidal
12	67/F	Bitemporal hemianopsia	15 × 14 × 16	Intrasellar and suprasellar	Transsphenoidal
13	67/F	No (with growth hormone macroadenoma)	13 × 13 × 22	Intrasellar and suprasellar	Transsphenoidal
14	58/F	Bitemporal hemianopsia	16 × 18 × 24	Intrasellar and suprasellar	Transsphenoidal
15	17/M	No	19 × 17 × 14	Intrasellar and suprasellar	Transsphenoidal
16	74/M	No	20 × 16 × 18	Intrasellar and suprasellar	Transsphenoidal
17	48/F	No (with chronic hypophysitis)	9 × 10 × 7	Intrasellar	Transsphenoidal
18	22/M	Diabetes insipidus	6 × 10 × 4	Intrasellar	Transsphenoidal

headache in two. Of the remaining four patients, one (case 13) was complicated by a growth hormone-producing macroadenoma, another (case 17) with chronic hypophysitis without symptoms. Two Rathke cleft cysts (cases 15 and 16) were incidentally found by MR imaging.

The MR scanners used were of low magnetic field strength (0.1 T) in four patients (cases 1 to 4), intermediate magnetic field strength (0.5 T) in four patients (cases 5 to 8), and high magnetic field strength (1 T or 1.5 T) in 10 patients (Table 2). In low magnetic field (0.1 T), T1-weighted inversion recovery (repetition time 500, inversion time 300, 2 excitations) images and T2-weighted spin-echo (1500–2000/80–120/1 [repetition time/echo time/excitations]) imaging were obtained with a 256 × 192 matrix, a field of view of 25 cm, a 5- to 10-mm section thickness, and no gap. In intermediate magnetic field strength, T1-weighted spin-echo (400–500/11–30/2) images and T2-weighted spin-echo (1800–2000/80–100/2) images were obtained with a 256 × 192 matrix, a field of view of 25 cm, a 5- to 7-mm section thickness, and no gap. In high magnetic field strength, T1-weighted spin-echo (400/11/4) images and T2-weighted spin-echo (2000–2100/80–100/2) images were obtained with a 256 × 128 matrix, a field of view of 14 cm, a 3-mm section thickness, and a 1-mm gap. Gadopentetate dimeglumine (Nihon Schering, Osaka, Japan) was injected in 15 patients. Coronal or sagittal T2-weighted imaging was performed, followed by coronal and sagittal T1-weighted imaging. Immediately after intravenous injection of 0.1 mm/kg of gadopentetate dimeglumine, coronal and sagittal T1-weighted imaging was done and, when necessary, axial imaging also.

Cyst intensity before surgery was compared with the intraoperative appearance of the cyst fluid, and contrast enhancement on MR was noted. The positions of the normal pituitary gland with respect to the tumor were also observed.

Results

The maximum diameters of the Rathke cleft cysts were 12 to 28 mm. The location was intrasellar in three patients, suprasellar in one, and intrasellar and suprasellar in the remaining 14 patients. Details of the radiographic and surgical findings are summarized in Table 2.

MR Findings

Cyst Intensity (Table 3). Eight patients had cysts with low intensity relative to white matter on T1-weighted images and high intensity on T2-weighted images (Figs 1 and 2). Ten patients had cysts with isointensity to high intensity on T1-weighted images, and variable intensity (four low, one iso, and five high) on T2-weighted images (Figs 3 and 4). No cysts showed low intensity on both T1- and T2-weighted images.

Nodular Intensity. In three patients (cases 7, 15, and 16), an intracystic nodule was identified based on different signal intensity from surrounding cyst fluid. The nodules appeared high intensity on T1-weighted images and low intensity on T2-weighted images (Fig 2).

TABLE 2: Radiographic and surgical findings in 18 Rathke cleft cysts

Case	Magnetic Field Strength (T)	MR Findings			CT Findings		Surgical Findings	
		Cyst Intensity		Gadopentetate Dimeglumine	Cyst Density	Enhancement	Cyst Fluid	Position of Normal Pituitary Gland
		T1-weighted	T2-weighted					
1	0.1	Low	High	Not done	Low	No	Light brown	Posterior
2	0.1	Low	High	Not done	Low	No	Milky	Anterior
3	0.1	Low	High	Not done	Low	No	Cerebrospinal fluid-like	Inferior
4	0.1	Low	High	No	Iso	No	Cerebrospinal fluid-like	No shift
5	0.5	High	Low	Surrounding	Iso	Ring-like	Thick milky	Surrounding
6	0.5	Low	High	Inferior	Iso	No	Milky	Inferior
7	0.5	High	Low	Anterior	High	No	Inferior thick milky	Anterior
		Low	High		Iso		Superior light brown	
8	0.5	Low	High	Inferior	Iso	No	Cerebrospinal fluid-like	Inferior
9	1	Iso	High	Anterior	High	No	Milky	Anterior
10	1	Iso	Low	Surrounding	High	Ring-like	Thick milky	Surrounding
11	1.5	High	High	Superior	High	Ring-like	Thick milky	Superior
12	1.5	High	Iso	Inferior	High	No	Thick milky	Inferior
13	1.5	Low	High	Anterior	Low	No	Motor oil-like	Anterior
14	1.5	High	Low	Surrounding	Iso	Ring-like	Thick milky	Surrounding
15	1.5	High	High	Anterior	High	No	Thick milky	Anterior
		High	Low		High		Superior waxy nodule	
16	1.5	High	High	Anterior	High	No	Thick milky	Anterior
		High	Low		High		Center waxy nodule	
17	1.5	Iso	Low	Surrounding	Low	Ring-like	Thick milky	Surrounding
18	1.5	High	High	Anterior	Iso	No	Thick milky	Anterior

TABLE 3: Cyst intensity in 18 Rathke cleft cysts

		T2-weighted		
	Intensity	Low	Iso	High
T1-weighted	Low	0	0	8
	Iso	2	0	1
	High	2	1	4

Enhancement. Enhancement with gadopentetate dimeglumine was observed in the cyst circumferences of 14 out of 15 patients. The sites of enhancement were variable: inferior in three patients (Fig 1), anterior in six (Fig 2), superior in one (Fig 3), and surrounding the tumor in four patients (Fig 4). These sites were clearly identified on sagittal images and correspondent to the normal pituitary gland in all patients (see below).

Surgical Findings

Thirteen patients had transsphenoidal surgery, and the remaining five had transcranial surgery. In all cases with transcranial surgery, the preoperative diagnosis was craniopharyngioma. Total surgical excision was performed in two patients (cases 4 and 10), and aspiration of cyst fluid with partial resection of the cyst wall was performed in the remaining 16 patients. The appearance of the cyst fluid and the position of the normal pituitary gland was identified during surgery in all patients. The normal pituitary gland was reddish tough tissue and was easily differentiated from the cyst wall.

The fluid of the cyst with low-intensity T1-weighted images and high-intensity T2-weighted images was cerebrospinal fluid–like or light brown in five patients, motor oil–like in one, and milky in two. The fluid of the cyst with isointensity to high-intensity T1-weighted images and variable T2-weighted images was milky in all 10 cases. No hemorrhagic fluid was observed.

In two of three patients with different nodular intensity regions (cases 15 and 16), a yellow waxy solid mass was found at a site that showed high intensity on T1-weighted images and low intensity on T2-weighted images. In the other patient (case 7), thick milky fluid was found within light brown fluid.

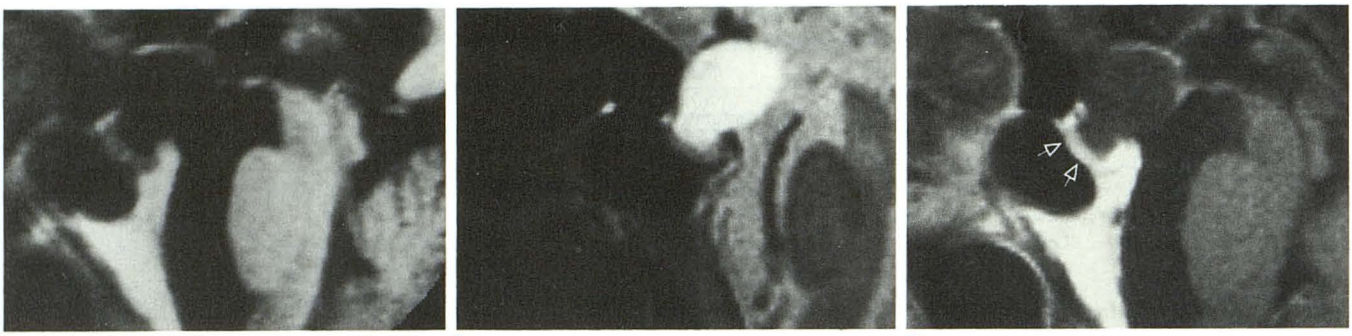

Fig. 1. Case 6, a 20 × 16 × 23-mm cyst that contained milky fluid.
A, T1-weighted sagittal inversion-recovery image (repetition time 2000, inversion time 600) demonstrates a low-intensity cyst.
B, T2-weighted sagittal spin-echo image (2000/100) demonstrates a high-intensity cyst.
C, Gadolinium-enhanced sagittal spin-echo image (400/26) demonstrates a nonenhanced cyst and the strongly enhanced normal pituitary gland (*arrows*) compressed inferior to the cyst.

The position of the normal pituitary gland was identified during surgery and was consistent with the site where enhancement was observed. The position of the normal pituitary gland was variable in our 18 patients: inferior in four patients, anterior in seven patients, superior in one patient, surrounding the tumor in four patients, posterior in one patient, and not displaced in one patient. In a patient in whom enhancement was not seen, it was confirmed that the cyst was located in the suprasellar cistern, and that the normal pituitary gland was not displaced. The normal pituitary gland was identified in only eight of 15 patients when nonenhanced T1-weighted images were used alone (Figs 3 and 4).

Pathologic Findings

Histologic examinations of the tumor specimens were performed by a single neuropathologist. Tumor fragments were fixed for classical histologic study and stained using the hematoxylin and eosin method. A single layer of cuboidal or columnar epithelium was found in all patients. In 12 patients, cilia was found. In eight patients, goblet cells were found. Stratified squamous epithelium was found in three patients (cases 5, 6, and 8). Inflammatory cells were found only in two patients, one of which had chronic hypophysitis (cases 6 and 18).

Some biopsies of the normal pituitary glands were obtained in 10 patients (cases 5, 7, and 11 to 18) and were confirmed pathologically.

Discussion

The most common theory on the origin of Rathke cleft cysts is that they are derived from remnants of the embryologic Rathke pouch (7). The epithelium of Rathke cleft is a vestige of Rathke pouch, an embryonic upward growth of ectoderm from the stomodeum or primitive oral cavity. Rathke pouch is the precursor of the anterior lobe, intermediate lobe, and pars tuberalis of the pituitary gland. Rathke pouch has anterior and posterior walls and a central embryonic cleft. The anterior wall of the pouch proliferates to form the anterior lobe of the pituitary gland and the pars tuberalis; the posterior wall becomes the pars intermedia. The residual lumen of the pouch is reduced to a narrow Rathke cleft, which generally regresses. It is the persistence and enlargement of this cleft that is said to be the cause of the symptomatic Rathke cleft cyst. Other authors have different theories for the formation of Rathke cleft cysts and have suggested that the cells of origin may be derived from neuroepithelium (8), metaplastic anterior pituitary cells (9), or endoderm (10).

Diagnosis of sellar and juxtasellar tumors can be made by simple skull radiographs, cerebral angiography, CT, or MR imaging. However, it has been difficult to diagnose Rathke cleft cyst before surgery, even by MR. Gadopentetate dimeglumine has become clinically available in recent years as a contrast medium for MR imaging, and the ability to diagnose tumors by MR has improved. We report a comparison of CT and gadopentetate dimeglumine–enhanced MR imaging of Rathke cleft cyst with surgical findings.

In this study of 18 patients, eight patients had cysts with low intensity on T1-weighted images and high intensity on T2-weighted images. Ten patients had cysts with isointensity to high intensity on T1-weighted images and variable intensity

on T2-weighted images. Three patients had nodules within cysts, which showed high intensity on T1-weighted images and low intensity on T2-weighted images.

Thirty-two patients previously have been analyzed with respect to cyst intensity (6, 11–22). When our 18 patients are added to those patients, the following observation regarding MR intensities of the cysts emerge: 37 of 50 patients have cysts with homogeneous intensity. Cysts display a variety of intensities: low intensity on T1-weighted images and high intensity on T2-weighted images in 16 patients, isointensity or high intensity on T1-weighted images and isointensity or low intensity on T2-weighted images in 18 patients; isointensity or high intensity on T1-weighted images and high intensity on T2-weighted images in nine patients; low intensity on both T1-weighted and T2-weighted images in two patients; and in the remaining five patients isointensity or high intensity only on T1-weighted images. In 16 patients who displayed low intensity on T1-weighted images and high intensity on T2-weighted images, the cyst fluid was cerebrospinal fluid–like or light brown in 14 patients and milky in two. The cyst fluid in 32 patients with isointensity or high intensity on T1-weighted images was milky in 29 patients, hemorrhagic in two, and dark brown in one. Thirteen patients have a nodular intensity region within cysts on both T1-weighted and T2-weighted images. These included regions with isointensity or high intensity on T1-weighted images. The cyst fluid in 12 patients was milky, and five cysts included a "waxy nodule," referred to as such by Kucharczyk et al (12). On the basis of the above-mentioned observations, all cases were classified into three types as follows: 1) low intensity on T1-weighted images; and high intensity on T2-weighted images, cerebrospinal fluid–like or light brown cyst fluid; 2) isointensity or high intensity on T1-weighted images and variable intensity on T2-weighted images, milky cyst fluid; and 3) heterogeneous intensity on MR imaging, milky cyst fluid with a waxy nodule. Therefore, the diagnosis of Rathke cleft cysts is not possible by cyst intensity on MR imaging alone (23).

The cause of the variable cyst intensities is not known, but the presence of cholesterol (12,16) and mucopolysaccharide (16) content has been suspected. Ahmadi et al reported that cholesterol had no effect and protein concentration had large effect on cyst intensity on T1-weighted images in craniopharyngioma (24). Dillon et al have reported reduction in intensity of sinus secretion at a 25% macromolecular concentration or above (25). However, because cyst intensity of Rathke cleft cysts was variable, it is impossible to explain

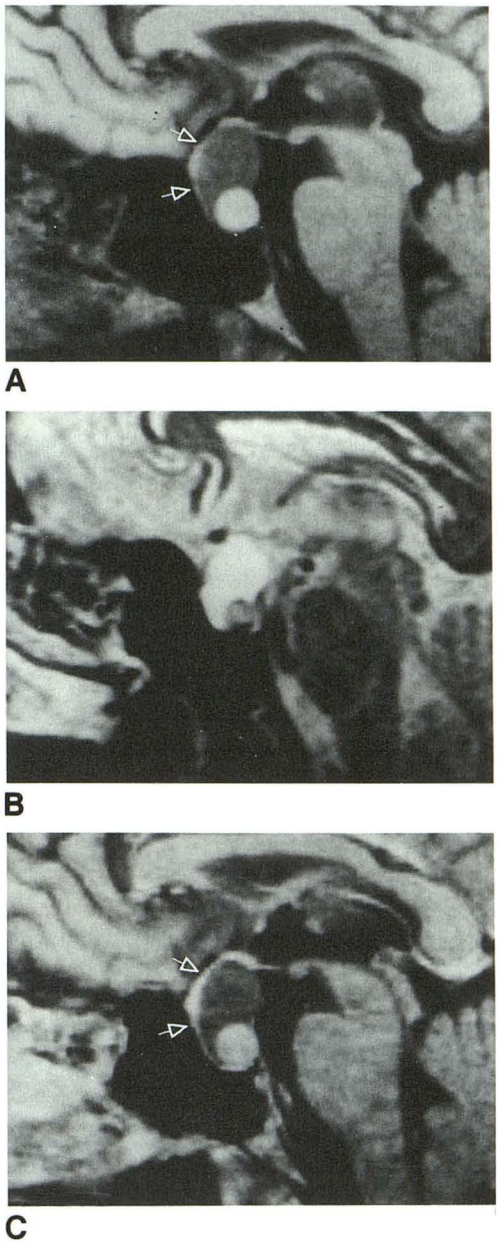

Fig. 2. Case 7, a 16 × 15 × 22-mm cyst in which two entirely different cystic components were found. One (the superior portion of the cyst) contained light brown fluid; the other (the inferior portion of the cyst) contained milky fluid.

A, T1-weighted sagittal spin-echo image (400/14) demonstrates a low-intensity suprasellar lesion and a high-intensity intrasellar lesion with the isointense normal pituitary gland compressed anterior to the cyst (*arrows*).

B, T2-weighted sagittal spin-echo image (2000/100) demonstrates a high-intensity suprasellar lesion and a low-intensity intrasellar lesion.

C, Gadolinium-enhanced sagittal spin-echo image (400/14) demonstrates a nonenhanced cyst and the enhanced normal pituitary gland (*arrows*).

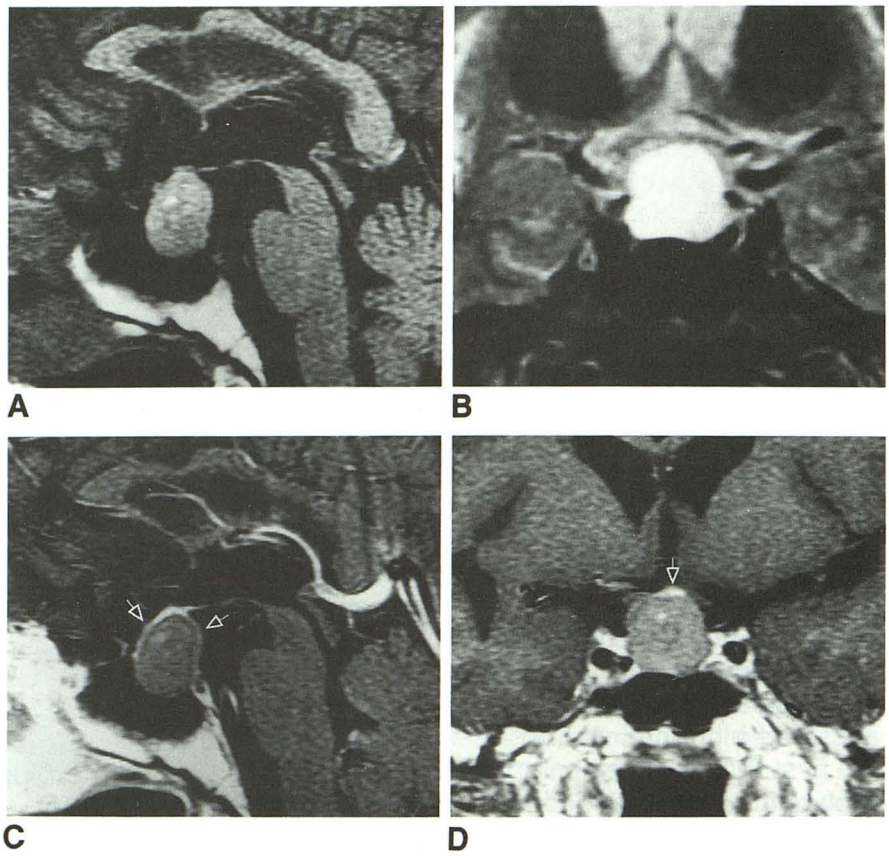

Fig. 3. Case 11, a 17 × 16 × 18-mm cyst that contained thick milky fluid.

A, T1-weighted coronal spin-echo image (400/11) demonstrates a slightly high-intensity cyst.

B, T2-weighted coronal spin-echo image (2000/80) demonstrates a high-intensity cyst.

C, Gadolinium-enhanced sagittal spin-echo image (400/11) demonstrates the enhanced normal pituitary gland (*arrows*) compressed superior to the cyst.

D, Gadolinium-enhanced sagittal spin-echo image (400/11) demonstrates the enhanced normal pituitary gland (*arrows*) compressed superior to the cyst.

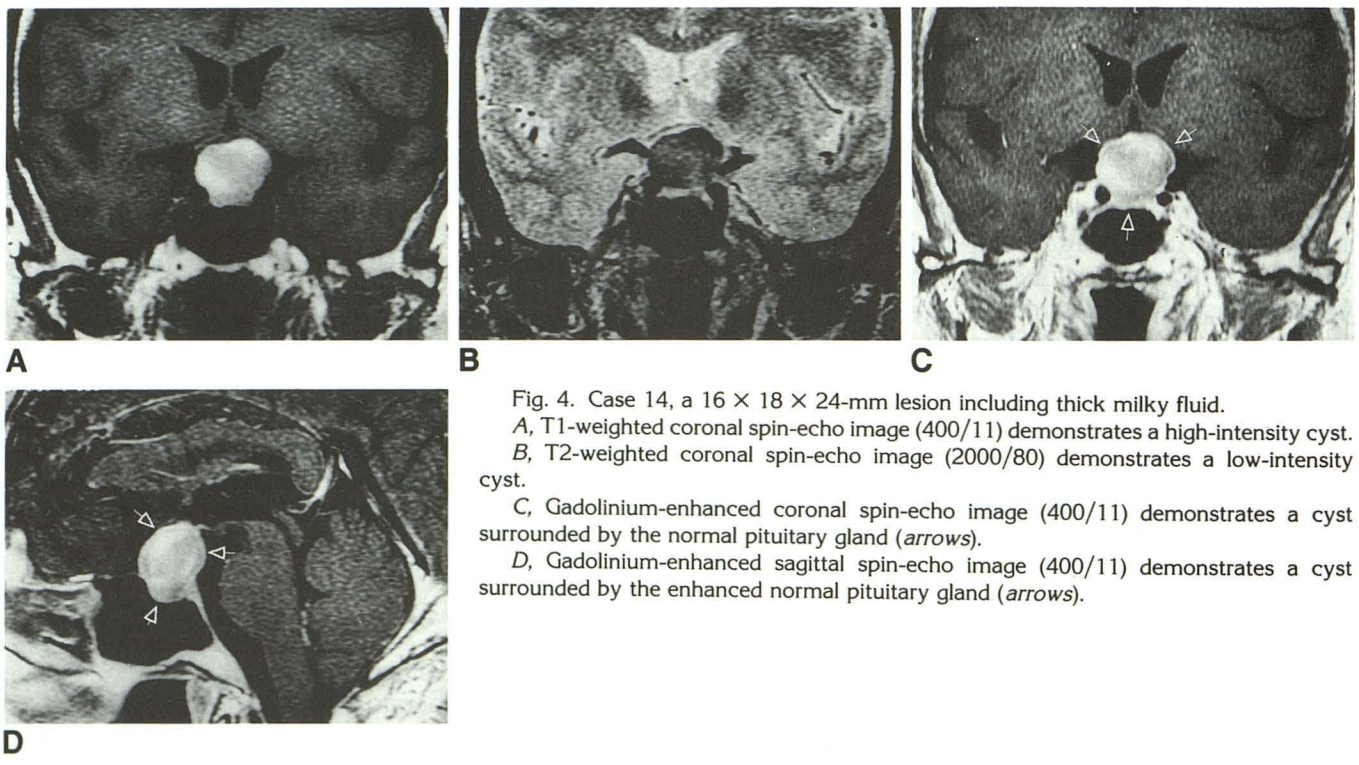

Fig. 4. Case 14, a 16 × 18 × 24-mm lesion including thick milky fluid.

A, T1-weighted coronal spin-echo image (400/11) demonstrates a high-intensity cyst.

B, T2-weighted coronal spin-echo image (2000/80) demonstrates a low-intensity cyst.

C, Gadolinium-enhanced coronal spin-echo image (400/11) demonstrates a cyst surrounded by the normal pituitary gland (*arrows*).

D, Gadolinium-enhanced sagittal spin-echo image (400/11) demonstrates a cyst surrounded by the enhanced normal pituitary gland (*arrows*).

the etiology with one material. Moreover, because the components of the milky cyst fluid are impossible to analyze and mucopolysaccharides cannot be quantified, this remains speculative.

Ring-like enhancement has been reported on CT in about half of the patients with Rathke cleft cysts (6). Compressed surrounding normal pituitary gland (26) or stratified squamous epithelium or inflammation (27) have been postulated to be responsible. Because gadopentetate dimeglumine does not enhance normal arteries or dura on MR (28, 29), and sagittal imaging is able to eliminate without interference by bone, accurate enhancement effects of the tumor can be evaluated. We showed that only the normal pituitary gland was enhanced by gadopentetate dimeglumine on MR imaging. In two of three patients with stratified squamous epithelium, enhancement was observed only in the site of the normal pituitary gland inferior to the cyst. Inflammatory cells were observed only in two patients, one of whom had chronic hypophysitis, the other of whom had no enhancement without the normal pituitary gland inferior to the cyst. These results were consistent with previous reports (26).

The position of the normal pituitary gland was variable in our 18 patients. Various possible origins for Rathke cleft cysts have been proposed, such as residual Rathke pouch (7), neuroepithelium derivation (8), abnormal differentiation of cells of the anterior lobe of the hypophysis (9), or abnormal appearance of endodermal tissue (10). However, because of the variety of positions with respect to the tumors noted here, we suggest that Rathke cleft cyst is derived from the anterior lobe, pars intermedia, posterior lobe, or infundibulum.

Important tumors in the differential diagnosis of Rathke cleft cyst include cystic craniopharyngiomas and cystic/hemorrhagic pituitary adenomas. Because only partial removal of a Rathke cleft cyst is regarded to be sufficient, with few recurrences reported (6), preoperative differentiation between craniopharyngioma or pituitary adenoma and Rathke cleft cyst is important. Based on the current study, the following comparisons can be drawn: 1) most cystic craniopharyngiomas have high intensity on T2-weighted images (30, 31); some Rathke cleft cysts do not show high intensity; 2) most cystic craniopharyngiomas have homogeneous intensity on MR imaging (30, 31), whereas Rathke cleft cysts have variable low or high intensities and are homogeneous or heterogeneous in appearance; 3) the normal pituitary gland is usually identified inferior to the tumor in craniopharyngiomas but is variable in Rathke cleft cysts, and tumor wall enhancement is observed in craniopharyngiomas, but not in Rathke cleft cysts (the enhancement seen represents the normal pituitary gland); and 4) calcification is frequently found on CT in craniopharyngiomas (32) but infrequently in Rathke cleft cysts (6). In pituitary adenomas, the position of the normal pituitary gland is usually superior to or surrounding the tumor, whereas the position is highly variable in Rathke cleft cysts; cyst wall enhancement is observed in pituitary adenoma; and the cyst wall is thick and irregular in pituitary adenomas but thin in Rathke cleft cysts (33, 34).

In conclusion, although Rathke cleft cyst occurs infrequently, preoperative distinction from other sellar and juxtasellar tumors is important, because prognosis and surgical management are different for this tumor. This task can be aided by noting the lack of tumor enhancement on MR with gadopentetate dimeglumine and the position of the normal pituitary gland with respect to this tumor.

Acknowledgments

We thank Tamotsu Kitaoka, MD, Hideki Satoh, MD, Fusao Ikawa, MD (Department of Neurosurgery, Hiroshima Prefectural Hospital), Junji Goishi, MD (Department of Neurosurgery, Matsuyama Red Cross Hospital), Katsuaki Sakoda, MD (Department of Neurosurgery, Mazda Hospital), Takeshi Shima, MD (Department of Neurosurgery, Chugoku Rousai Hospital), Mitsuo Yamamoto, MD (Department of Neurosurgery, Matsue Red Cross Hospital), and Toshio Kajima, MD (Department of Radiology, Hiroshima University School of Medicine) for allowing use of case materials. We thank William P. Dillon, MD (Department of Radiology, Neuroradiology Section, University of California, San Francisco) for valuable assistance.

References

1. Shanklin WM. On the presence of cysts in the human pituitary. *Anat Rec* 1949;104:399–407
2. Shanklin WM. The incidence and distribution of cilia in the human pituitary with a description of micro-follicular cysts derived from Rathke's cleft. *Acta Anat* 1951;11:361–382
3. Baskin DS, Wilson CB. Transsphenoidal treatment of non-neoplastic intrasellar cysts. *J Neurosurg* 1984;60:8–13
4. Fager CA, Carter H. Intrasellar epithelial cysts. *J Neurosurg* 1964;24:77–81
5. Hardy J, Vezina JL. Transsphenoidal neurosurgery of intracranial neoplasm. *Adv Neurol* 1976;15:261–274
6. Voelker JL, Campbell RL, Muller J. Clinical, radiographic, and pathological features of symptomatic Rathke's cleft cysts. *J Neurosurg* 1991;74:535–544

7. Frazier CH, Alpens BJ. Tumors of Rathke's cleft (hitherto called tumors of Rathke's pouch). *Arch Neurol Psychiatry* 1934;32:972–984
8. Shuangshoti S, Netsky MG, Nashold BSJ. Epithelial cysts related to sella turcica. *Arch Pathol* 1970;90:444–450
9. Rasmussen AT. Ciliated epithelium and mucus secreting cells in the human hypophysis. *Anat Rec* 1929;41:273–283
10. Hirano A, Ghatak NR, Wisoff HS, et al. An epithelial cyst of the spinal cord, and electron microscopic study. *Acta Neuropathol (Berl)* 1971;18:214–223
11. Asari S, Ito T, Tsuchida S, et al. MR appearance and cyst component of Rathke's cleft cysts. *J Comput Tomogr* 1990;14:532–535
12. Kucharczyk W, Peck WW, Kelly WM, et al. Rathke's cleft cysts: CT, MR imaging, and pathologic features. *Radiology* 1987;165:491–495
13. Ito H, Shoin K, Hwang WZ, et al. Preoperative diagnosis of Rathke's cleft cyst. *Childs Nerv Syst* 1987;3:225–227
14. Ishii T, Yamasaki T, Tanaka J, et al. Rathke's cleft cyst. Report of three cases. *No Shinkei Geka* 1987;15:451–456
15. Maggio WW, Cail WS, Brookeman JR, et al. Rathke's cleft cyst: computed tomographic and magnetic resonance imaging appearance. *Neurosurgery* 1987;21:60–62
16. Nemoto Y, Inoue Y, Fukuda T, et al. MR appearance of Rathke's cleft cysts. *Neuroradiology* 1988;30:155–159
17. Murata J, Aida T, Miyamachi K, et al. A neuroradiological study of Rathke's cleft cyst. *Prog Comput Tomogr (Jpn)* 1988;10:161–165
18. Wagle VG, Nelson D, Rossi A, et al. Magnetic resonance imaging of symptomatic Rathke's cleft cyst: report of a case. *Neurosurgery* 1989;24:276–278
19. Onda K, Tanaka R, Takeda N, et al. Symptomatic Rathke's cleft cyst simulating arachnoid cyst. *Neurol Med Chir (Tokyo)* 1989;29:1039–1043
20. Onesti ST, Wiswskinie T, Post KD. Pituitary hemorrhage into a Rathke's cleft cyst. *Neurosurgery* 1990;27:644–646
21. Yuge T, Shigemori M, Tokutomi T, et al. Entirely suprasellar symptomatic Rathke's cleft cyst. *No Shinkei Geka* 1991;19:273–278
22. Midha R, Jay V, Smyth HS. Transsphenoidal management of Rathke's cleft cysts: a clinicopathological review of 10 cases. *Surg Neurol* 1991;35:446–454
23. Ross DA, Norman D, Wilson CB. Radiologic characteristics and results of surgical management of Rathke's cysts in 43 patients. *Neurosurgery* 1992;30:173–179
24. Ahmadi J, Destian S, Apuzzo MJ, et al. Cystic fluid in craniopharyngiomas: MR imaging and quantitative analysis. *Radiology* 1992;182:783–785
25. Dillon WP, Som PM, Fullerton GD. Hypointense MR signal in chronically inspissated sinonasal secretions. *Radiology* 1990;174:73–78
26. Dietemann JL, Bonneville JF, Buchheit F, et al. CT findings in symptomatic Rathke's cleft cysts of the pituitary gland. Report of three cases. *Neuroradiology* 1983;24:263–267
27. Okamoto S, Handa H, Yamashita J, et al. Computed tomography in intra- and suprasellar epithelial cysts (symptomatic Rathke's cleft cysts). *AJNR Am J Neuroradiol* 1985;6:515–519
28. Kilgore DP, Breger RK, Daniels DL, et al. Cranial tissues: normal MR appearance after intravenous injection of Gd-DTPA. *Radiology* 1986;160:757–761
29. Bronen RA, Sze G. Magnetic resonance imaging contrast agents: theory and application to the central nervous system. *J Neurosurg* 1990;73:820–839
30. Freeman MP, Kessler RM, Allen JH, et al. Craniopharyngioma: CT and MR imaging in nine cases. *J Comput Assist Tomogr* 1987;11:810–814
31. Pusey E, Kortman KE, Flannigan BD, et al. MR of craniopharyngiomas: tumor delineation and characterization. *AJR Am J Roentgenol* 1987;149:383–388
32. Cabezodo JM, Vaguero J, Garcia de Sola, et al. Computed tomography with craniopharyngiomas: a review. *Surg Neurol* 1981;15:422–427
33. Post JD, David NJ, Glaser JS, et al. Pituitary apoplexy: diagnosis by computed tomography. *Radiology* 1980;134:665–670
34. Ostrov SG, Quencer RM, Hoffman JC, et al. Hemorrhage within pituitary adenomas: how often associated with pituitary apoplexy syndrome? *AJNR Am J Neuroradiol* 1989;10:503–505